

図7. 糖尿病性腎症血清サンプルの主成分分析 (PCA) 結果

○：糖尿病性腎症Ⅰ期（腎症前期）、△：糖尿病性腎症Ⅱ期（早期腎症期）、◇：糖尿病性腎症Ⅲ期（顕性腎症期）、◎：糖尿病性腎症Ⅳ期（腎不全期）

Symmetric dimethylarginine (SDMA) やキヌレニンといった、これまで腎障害と相関があると知られているいくつかの既知のマーカーを検出することができた(図6)。また、有意差のみられたすべてのピークを用いて主成分分析を行った結果(図7)、Ⅰ期とⅡ期の分離は不明瞭であったが、病期の進行に伴い各サンプルのプロットが第一主成分に対して正方向へシフトすることがわかり、メタボロームデータからも病期の推測が可能であることが示唆された。

おわりに

筆者らはこれまでに、CE-MS法をさまざまなサンプルに適用し、興味深い知見を得ることができた。しかしながら、CE-MSに限らずメタボローム測定で得られる膨大なピークのうち、同定できるのはせいぜい3割程度であり、残りの

ピークについては手つかずになっているのが現状である。分析化学的な側面から、これらのピークの同定を進めてさらなるメタボロミクスの発展に寄与できれば幸いである。

謝辞

本研究は、名古屋大学医学部腎臓内科 丸山彰一先生、秋山真一先生、藤田保健衛生大学医学部腎内科学 湯澤由紀夫先生、ならびに中部ろうさい病院 中島英太郎先生との共同研究の一部である。

また本研究は、山形県および鶴岡市の支援によるものである。

文献

1. Soga T, Ohashi Y, Ueno Y, et al : Quantitative metabolome analysis using capillary electrophoresis mass spectrometry. *J Proteome Res* 2 : 488-494, 2003
2. Ohashi Y, Hirayama A, Ishikawa T, et al : Depiction of metabolome changes in histidine-starved *Escherichia coli* by CE-TOFMS. *Mol Biosyst* 4 : 135-147, 2008
3. Ishii N, Nakahigashi K, Baba T, et al : Multiple high-throughput analyses monitor the response of *E. coli* to perturbations. *Science* 316 : 593-597, 2007
4. Sato S, Soga T, Nishioka T, et al : Simultaneous determination of the main metabolites in rice leaves using capillary electrophoresis mass spectrometry and capillary electrophoresis diode array detection. *Plant J* 40 : 151-163, 2004
5. Hirayama A, Kami K, Sugimoto M, et al : Quantitative metabolome profiling of colon and stomach cancer microenvironment by capillary electrophoresis time-of-flight mass spectrometry. *Cancer Res* 69 : 4918-4925, 2009
6. Soga T, Baran R, Suematsu M, et al : Differential metabolomics reveals ophthalmic acid as an oxidative stress biomarker indicating hepatic glutathione consumption. *J Biol Chem* 281 : 16768-16776, 2006
7. Soga T, Heiger DN : Amino acid analysis by capillary electrophoresis electrospray ionization mass spectrometry. *Anal Chem* 72 : 1236-1241, 2000
8. Soga T, Igarashi K, Ito C, et al : Metabolomic profiling of anionic metabolites by capillary electrophoresis mass spectrometry. *Anal Chem* 81 : 6165-6174, 2009
9. Soga T, Ueno Y, Naraoka H, et al : Simultaneous determination of anionic intermediates for *Bacillus subtilis* metabolic pathways by capillary electrophoresis electrospray ionization mass spectrometry. *Anal Chem* 74 : 2233-2239, 2002
10. Baran R, Kochi H, Saito N, et al : MathDAMP: a package for differential analysis of metabolite profiles. *BMC Bioinformatics* 7 : 530, 2006
11. Baran R, Robert M, Suematsu M, et al : Visualization of three-way comparisons of omics data. *BMC Bioinformatics* 8 : 72, 2007
12. Sugimoto M, Wong DT, Hirayama A, et al : Capillary electrophoresis mass spectrometry-based saliva metabolomics identified oral, breast and pancreatic cancer-specific profiles. *Metabolomics* 6 : 78-95, 2010

新規酸化ストレスマーカーγ-グルタミルジペプチドによる肝疾患スクリーニング

曾我 朋義*・杉本 昌弘*・本間 雅**・斉藤 貴史***・末松 誠****

はじめに

各種の肝疾患患者から採取した血清中のメタボローム(低分子代謝物の総称)を網羅的に測定することによって、肝内のグルタチオン(GSH)の生合成量を示すγ-グルタミルジペプチド類を発見した。この新規の酸化ストレスに関するマーカーを1個から数個組み合わせることにより、薬剤性肝炎(DI)、B型肝炎持続感染(AHB)、B型慢性肝炎(CHB)、C型肝炎持続感染(CNALT)、C型慢性肝炎(CHC)、肝硬変(CIR)、肝細胞がん(HCC)患者を高い精度で診断できることがわかった。またこのマーカーにより単純性脂肪肝(SS)や非アルコール性肝炎(NASH)の区別も可能であることが示唆された。各種の肝臓疾患のスクリーニング法およびγ-グルタミルジペプチド類の生合成の機序について報告したい。

メタボローム測定によるマウスの薬剤性肝炎マーカーの発見

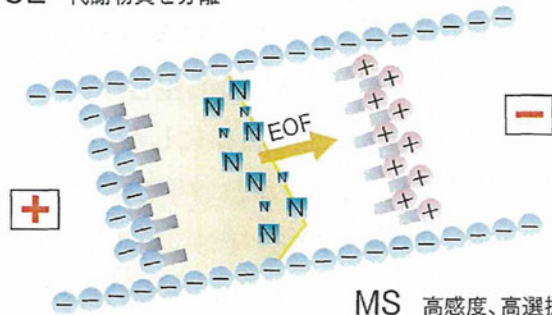
メタボローム解析は、細胞や生体試料に存在する低分子代謝物を網羅的に測定する方法論であり、代謝調節機構の解明、遺伝子やタンパク質の機能解明から疾患やがんの機序の解明、

病態の診断、各種バイオマーカーの探索などに有効な解決策を与えるのではないかと期待されている。

筆者らは、イオン性の低分子代謝物に対して、高分離能、高感度測定を可能にしたキャピラリー電気泳動-質量分析計(CE-MS)法(図1)を開発し¹⁾²⁾、細胞や組織に存在する1,000種類以上の代謝物の一斉分析を実現した。本法により、これまでに解熱鎮痛薬であるアセトアミノフェン(APAP)で惹起される急性肝炎の血中バイオマーカー(γ-glutamyl-2-aminobutyryl glycine; オフタルミン酸)を発見している(図2)²⁾。APAPをマウスに過剰投与し、肝と血中の代謝物質の変動をメタボローム測定したところ、急性肝炎発症時に、APAPの代謝で生じた毒性の高い

図1 キャピラリー電気泳動-質量分析計(CE-MS)によるイオン性代謝物の測定法

CE 代謝物質を分離



γ-Glutamyl dipeptides as new oxidative stress biomarkers for discrimination among different forms of liver disease

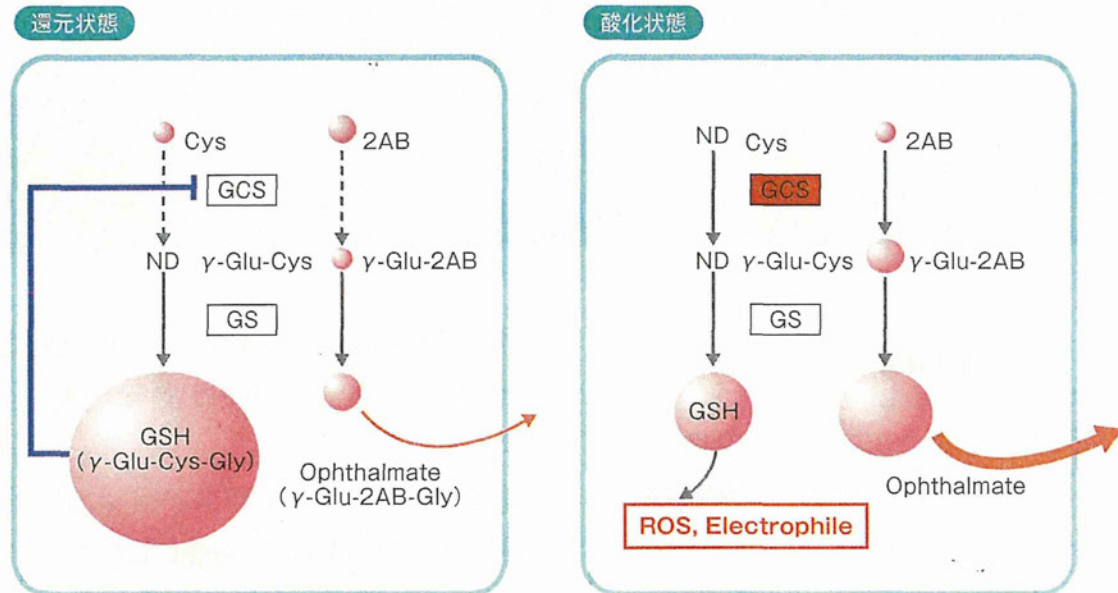
*SOGA Tomoyoshi et al 慶應義塾大学 先端生命科学研究所 [〒997-0052 山形県鶴岡市覚岸寺水上246-2]

**HONMA Masashi 東京大学 病院薬剤部

***SAITO Takafumi 山形大学医学部 消化器内科学

****SUEMATSU Makoto 慶應義塾大学医学部 医化学教室

図2 ROSや親電子物質でオフタルミン酸が生合成される機序(マウス)



GSHはCysを、オフタルミン酸は2-アミノ酪酸(2AB)を基質にしてGCSとGSの触媒によって生合成される。通常(還元状態)では、GSHが豊富に存在するため、GCSがフィードバック阻害されており、GSHもオフタルミン酸もほとんど産生されない。酸化ストレス状態では、ROSや親電子物質の除去のためにGSHが消費されるとフィードバック阻害が解除されGCSの活性が亢進し、GSHとオフタルミン酸が生合成される。蓄積されたオフタルミン酸は肝から血中に輸送される。

親電子物質(N-acetyl-p-benzoquinone imine; NAPQI) に対して解毒作用を持つGSHの枯渇に伴い、GSHアナログであるオフタルミン酸が肝および血清で急増することを見出し(図2)、その生合成経路および機序を解明した²⁾。

GSHは、γ-グルタミルシステインシンセターゼ(GCS)とグルタチオンシンセターゼ(GS)の二つの酵素によって、Cysから生合成されるトリペプチドである(図2)。筆者らは、生化学的な実験によって、オフタルミン酸もGSHと同じ二つの酵素(GCSとGS)によって、2-アミノ酪酸(2AB)から生合成されるトリペプチドであることを明らかにした。また薬剤性肝炎でオフタルミン酸が急増する機序も解明した。通常(図2還元状態)では、肝細胞内にGSHが大量に存在し、これがGSH合成の最初の酵素であるGCSをフィードバック制御するためGSHやオフタルミン酸の生合成は抑制されている。しかし、NAPQIなどの親電子物質や活性酸素(ROS)の解毒のためにGSHが消費されると(図2酸化状態)、フィードバック阻害が解除されること

によってGCSが活性化し、GSHおよびオフタルミン酸が生合成される。しかし、オフタルミン酸はGSHのようにSH基を有していないため、親電子物質や活性酸素とは反応せず肝細胞内に蓄積し最終的に血中に輸送される(図2)²⁾。血中のオフタルミン酸は、肝のGSHがどれだけ生合成されているかを示す新規マーカーであり、生合成の機序からも酸化ストレスに深く関与する物質である²⁾。

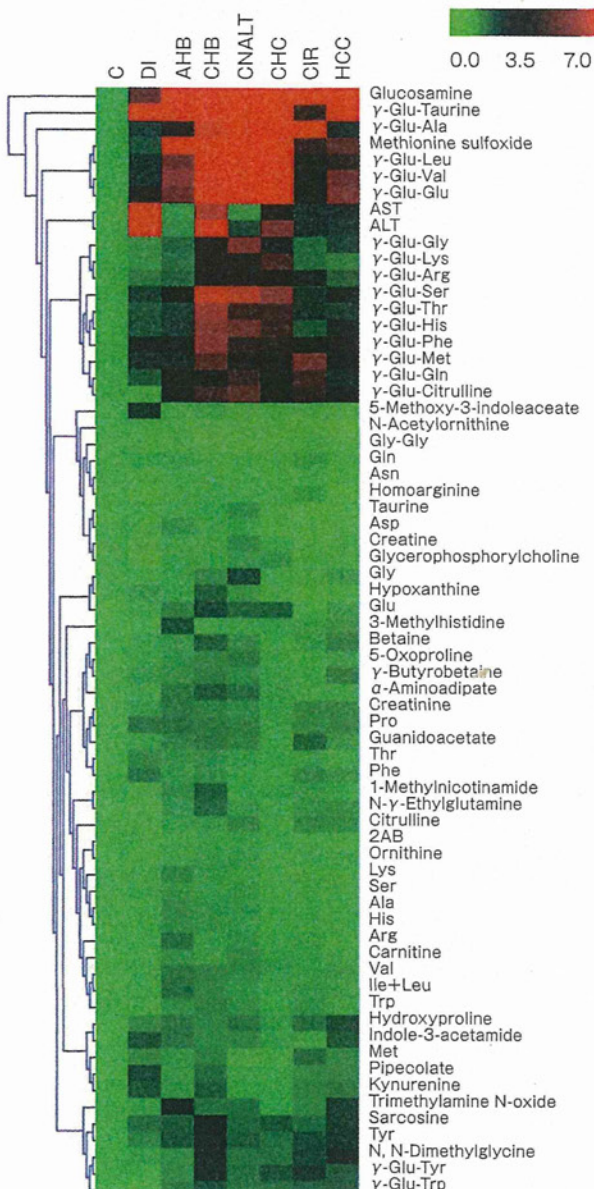
γ-グルタミルジペプチドの発見

多くの肝疾患で肝内のGSHの低下が認められており、マウスでは、オフタルミン酸は肝のGSHの生合成量を示すマーカーであった。そこでオフタルミン酸がヒトでも有用か確認するため、山形大病院(試験コホート)および東大病院(検証コホート)で得られた各種の肝疾患患者237例(DI 27例、AHB 16例、CHB 14例、CNALT 18例、CHC 35例、CIR 18例、HCC 32例、SS 9例、NASH 11例および健康成人(C) 57例)の血清中の

低分子代謝物をキャピラリー電気泳動-飛行時間型質量分析計(CE-TOFMS)によって網羅的に測定した³⁾。ヒートマップからわかるように、検出された代謝物のうち、健康成人に対し各種の肝疾患で10数種類の代謝物が高値を示した(図3)。高値を示した物質を得られた質量数情報および標準物質との比較から同定した結果、ほとんどが γ -グルタミルジペプチドであることが判明した。またグルコサミン⁴⁾、メチオニンスルフォキシド⁵⁾といった酸化ストレスに関与する物質

やAST、ALTも肝疾患で高値を示した。マウスではAPAPによる薬剤性肝炎でオフタルミン酸が有意に増加したが、ヒトの血清からはオフタルミン酸はほとんど検出されなかった。図4に試験コホートとして用いた各肝疾患のAST、ALT値と γ -グルタミルジペプチド、メチオニンスルフォキシド、グルコサミンの濃度の箱髭図を示した³⁾。AST、ALTは、DI、CHB、CHCなどで高値を示したが、B型、C型肝炎持続感染(AHB、CNALT)では、健康成人と有意な差はなかった。一方、 γ -グルタミルジペプチドのほとんどは、健康成人よりも肝疾患で有意に高い値を示した。メチオニンスルフォキシド、グルコサミンは、CHB、CNALT、CHCなどで高値を示した。

図3 各肝疾患患者の血清中の代謝物の濃度

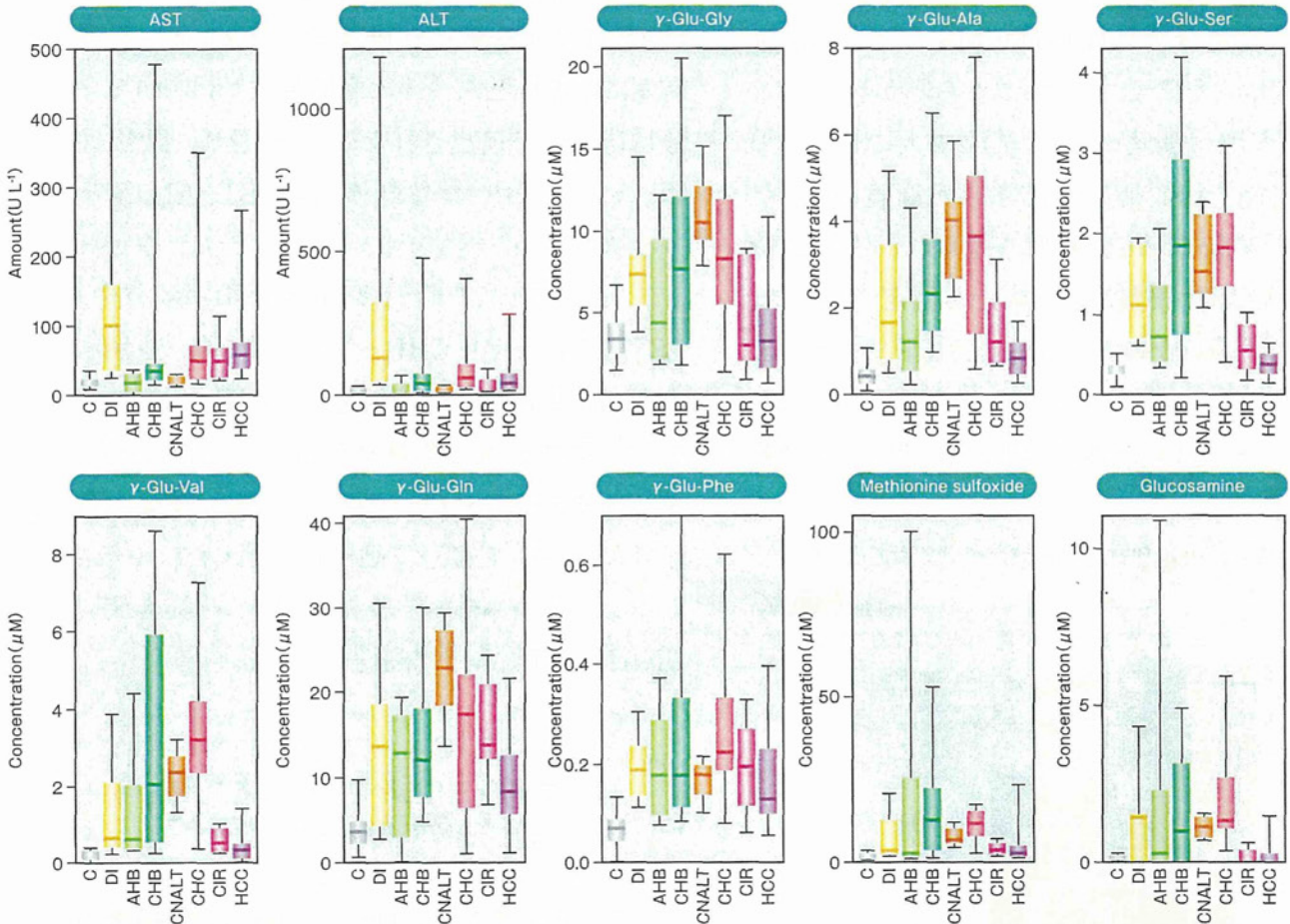


ほとんどの肝疾患で γ -グルタミルジペプチド類が高値を示した。

γ -グルタミルジペプチド類による肝疾患スクリーニング

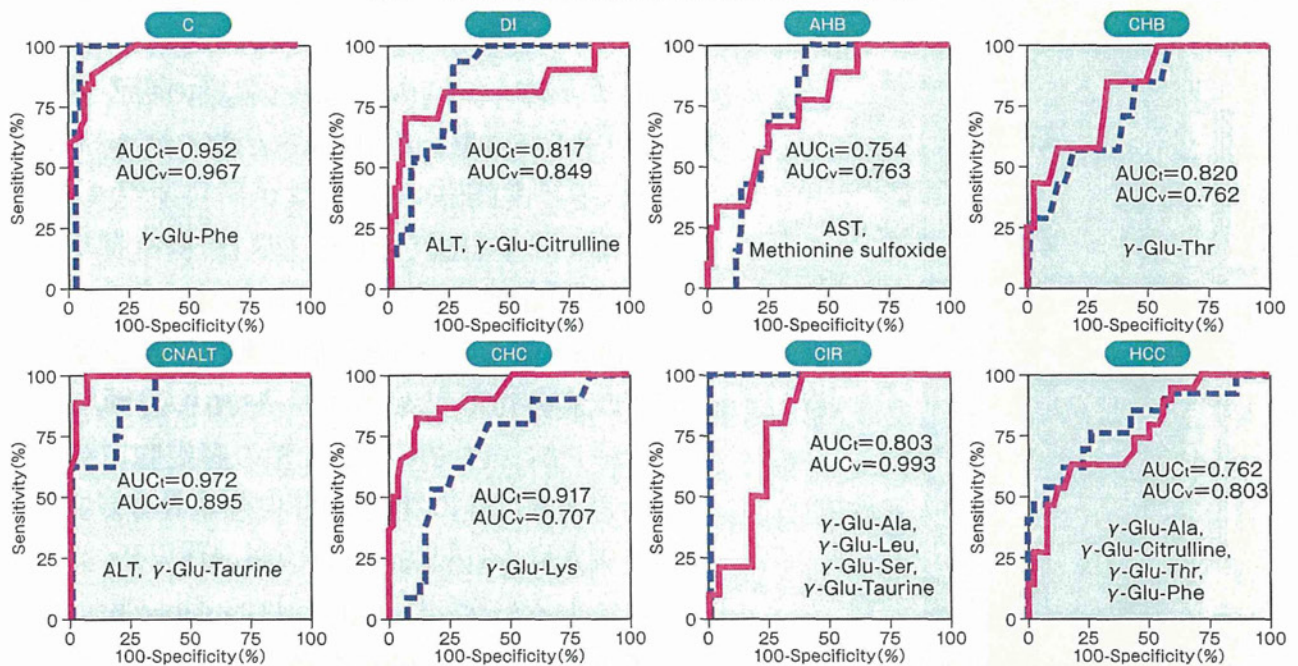
AST、ALTを含めた前述の物質は、肝疾患の種類に応じてそれぞれ特徴的な濃度を示した(図4)。そこで、筆者らは、幾つかの物質を組み合わせることにより、各肝疾患を判別できるのではないかと考えた。多変量解析の一つである多重ロジスティック回帰によって複数の物質を用いてある肝疾患を他の肝疾患と見分ける数理モデルを作成した(図5)。試験コホートを実線、検証コホートを点線で示した。例えば、健康成人を7種類の肝疾患患者から見分ける場合は、 γ -Glu-Pheの値を用いると受信者動作特性曲線以下の面積(AUC)は試験コホートで0.952、検証コホートで0.967であった。C型の肝細胞がん患者をそれ以外の6種類の肝疾患患者および健康成人から見分ける場合は、4種類の γ -グルタミルジペプチド(γ -Glu-Ala、 γ -Glu-Citrulline、 γ -Glu-Thr、 γ -Glu-Phe)の値を用いると試験コホートで0.762、検証コホートで0.803の精度で

図4 各肝疾患患者の血中の肝機能マーカーとγ-グルタミルジペプチド類などの濃度



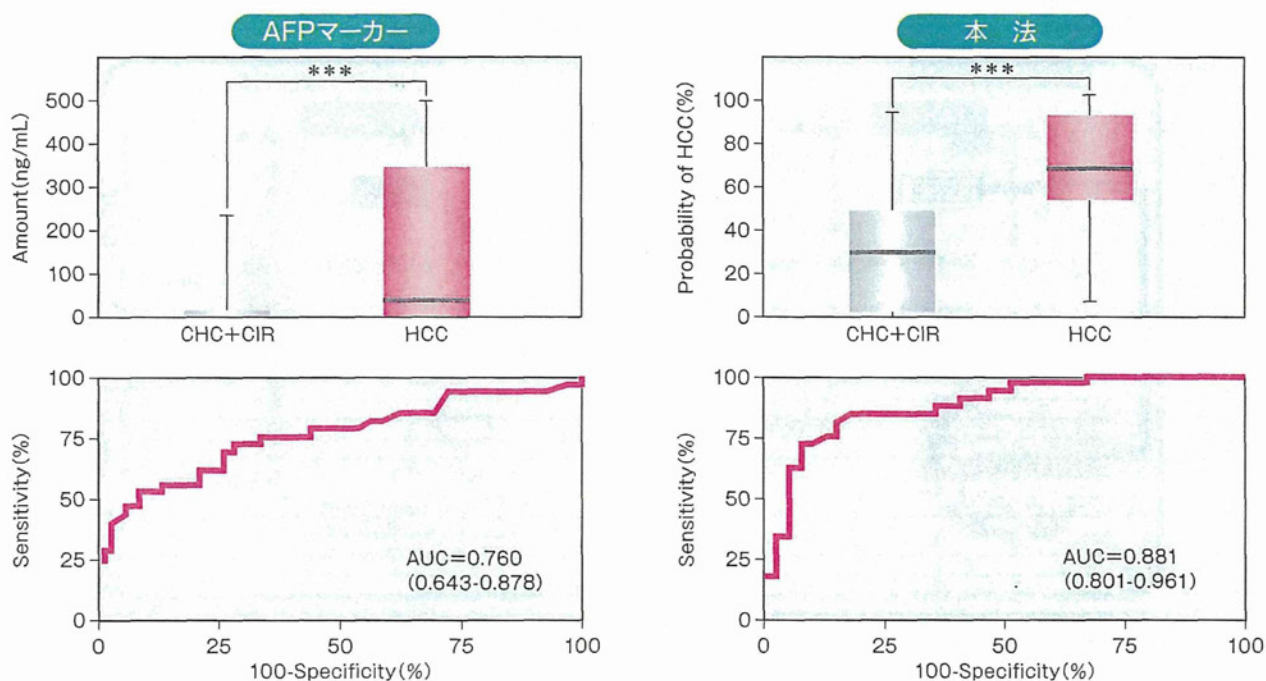
肝疾患によって、血中のγ-グルタミルジペプチド類の濃度が異なった。またγ-グルタミルジペプチド類の種類によって肝疾患に対する変動パターンが異なった。

図5 各肝疾患患者の受信者動作特性(ROC) 曲線



実線が試験コホート、点線が検証コホートのROC曲線を示した。AUCt、AUCvは、試験コホート、検証コホートの結果を示した。診断に用いたマーカーを各疾患のグラフに示した。

図6 肝細胞がんの診断精度の比較



CHC、CIRからHCCを診断する精度をAFPマーカーと比較した。本マーカー法の方が高いAUC値を示した。

あった。他の肝疾患もDI(試験コホート0.817、試験コホート0.849)、AHB(0.754、0.763)、CHBI(0.820、0.762)、CNALT(0.972、0.895)、CHC(0.917、0.707)、CIR(0.803、0.993)と高い精度で他の疾患と区別することができた³⁾。

次に、HCCをCHCとCIRからどのくらいの精度で見分けることができるか従来の肝がんマーカーであるα-fetoprotein(AFP)と比較した(図6)³⁾。AFPではAUC値は、0.760であるのに対して、本法で見出した4種類のγ-Glu-Ala、γ-Glu-Citrulline、γ-Glu-Thr、γ-Glu-Pheの値を用いると0.881の精度であり、本マーカーによる方法は、AFPよりも高い精度でHCCをCHCとCIRから見分けることができた。

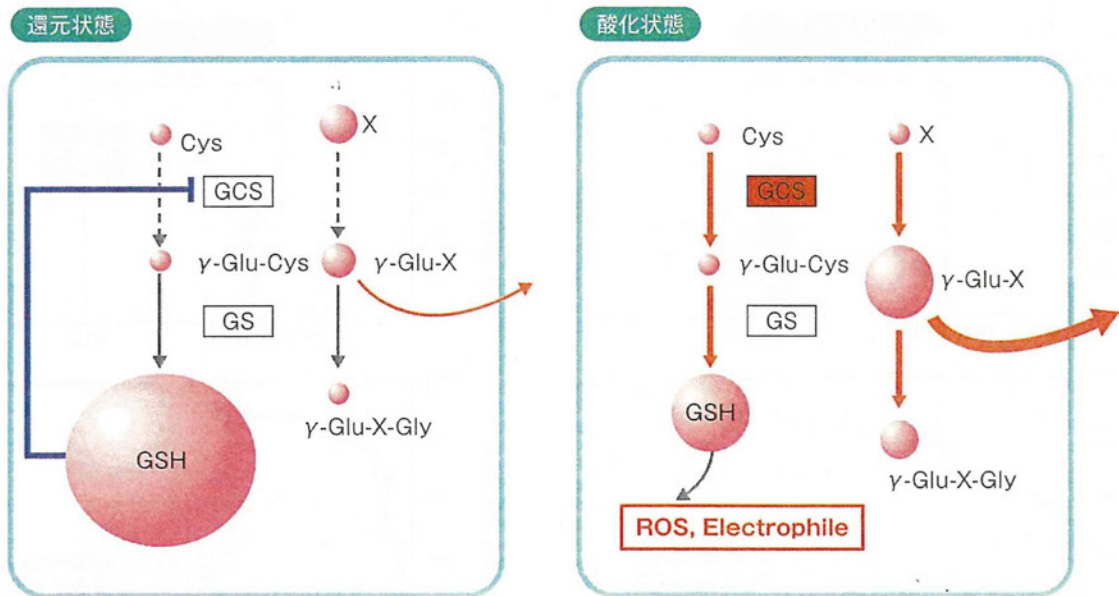
さらにγ-グルタミルジペプチド類の変動が肝疾患特異的かを検証するために胃がん患者から採取した血清を測定した。その結果、胃がん患者のγ-グルタミルジペプチド類の血中濃度は健康成人の値と同程度であることがわかった³⁾。GSHの生合成は肝が最も活発であるため、血中のγ-

グルタミルジペプチドは主に肝の変化を反映していると考えられる。

γ-グルタミルジペプチド類の生合成の機序の解明

前述のようにマウスでは、薬剤の代謝で生じた親電子物質によって消費されたGSHが新規に生合成される際に副産物としてγ-グルタミルトリペプチドであるオフタルミン酸が産生された(図2)²⁾。筆者らは、図7のようにγ-グルタミルジペプチド類も各種のアミノ酸やアミン(X)からGCSの触媒によって生合成されているのではないかと考えた。そこで、マウスを用いてGCSの働きを促進したり抑制したりする実験を行いγ-グルタミルジペプチド類の変動を測定し仮説を検証した。GCSの活性を阻害することが知られているブチオニンスルフォキシミン(BSO)⁶⁾をマウスに腹腔内投与し、肝のγ-グルタミルジペプチド類の濃度を測定したところ、多くのγ-グルタミルジペ

図7 酸化ストレスでγ-グルタミルジペプチド類が生合成される機序(ヒト)



ヒトの場合は酸化ストレス下で、肝でGCSの触媒によって各種のアミノ酸やアミン(X)からγ-グルタミルジペプチド類(γ-Glu-X)が生合成され、血中に輸送されることが分かった。

チド類が著しく減少した。一方、GCSの活性を促進することが知られているジエチルマレイン酸 (DEM)⁷⁾を投与すると、多くのγ-グルタミルジペプチド類は対象群に対して数倍から10数倍増加した。これらの結果は、γ-グルタミルジペプチド類がGCSによって触媒されていることを示唆した。さらに同位体ラベル標識されたスレオニンをマウスに腹腔内投与し、同時にAPAP投与による酸化ストレスを与えGCSの活性を亢進させたところ、スレオニン(Thr)が同位体ラベル標識されたγ-Glu-Thrが高濃度に検出された³⁾。以上の結果より、γ-グルタミルジペプチド類は、各種のアミノ酸やアミンを基質としてGCSの触媒によってグルタミン酸と結合してできたペプチドであることがわかった。γ-グルタミルジペプチド類は、親電子物質やROSなどの除去のためにGSHが生産されるとき副産物であり、その濃度はGSHの合成量を示唆することが明らかになった。GSHが生合成される際の副産物は、ヒトの場合はγ-グルタミルジペプチド類が多く、マウスはγ-グルタミルトリ

ペプチドのオフタルミン酸であった。この生物種間の副産物の違いの理由は不明であるが、代謝酵素やトランスポーターの濃度や活性がヒトとマウスでは異なっているのではないかと推測される。

NASH、SS診断の可能性

γ-グルタミルジペプチド類によってSSとNASHが区別できるか可能性を検討した³⁾。図8に示すようにNASHに比べSSでほとんどの血清中のγ-グルタミルジペプチド類は高値を示した。γ-グルタミルジペプチド類の濃度は、SS>NASH>CIR>Cであり、γ-Glu-Val、γ-Glu-Pheなど6種類のペプチドでNASHとSS間で有意な差が見られた(図9)。試験コホートのみのデータであるが、SSに関しては、γ-Glu-Leuの値を用いるとAUC0.957の精度で、SSをNASHや健康成人を含む他の肝疾患と見分けることができた。NASHは、γ-Glu-Thr、AST、ALTの値を用いると0.971の精度で、SSや健康成人を含む他の

図8 SSとNASH患者の血清中の γ -グルタミルジペプチド類の濃度の比較

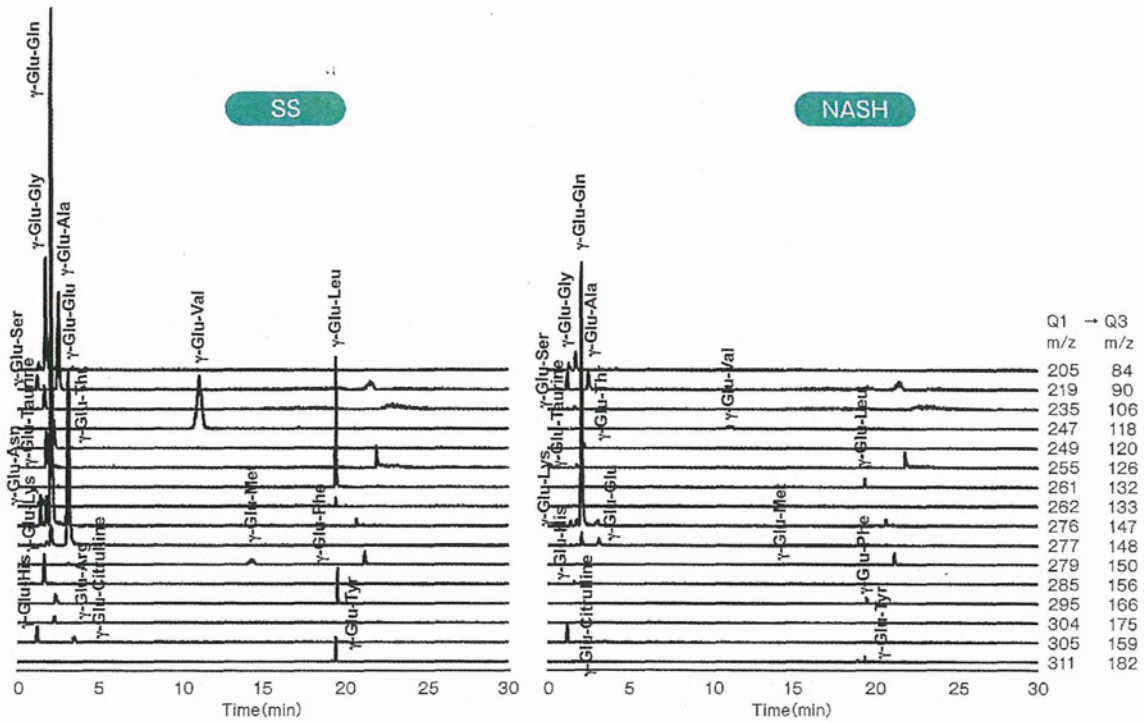
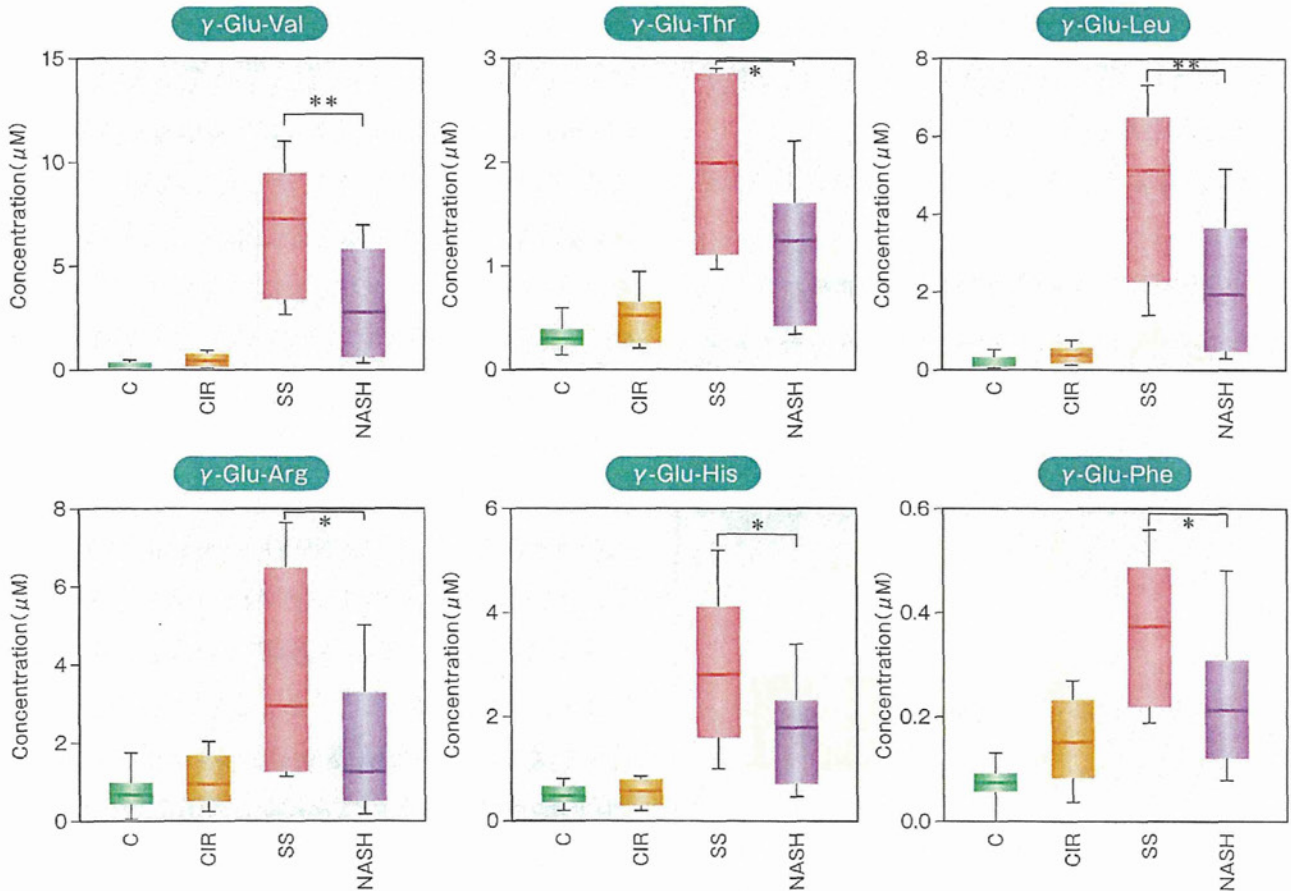


図9 健康成人とCIR、SS、NASH患者の血清中の γ -グルタミルジペプチド類の濃度の比較



肝疾患と見分けることができた。しかしSS9例、NASH11例と症例が少ないため、今後さらに多くの検体の測定を行い、このマーカーによる診断法の精度を検証することが必要である。

GSH生合成と肝疾患

酸化ストレスが肝疾患に密接に関与していることは広く知られている。酸化ストレスに対する生体の抗酸化物質としては、GSH、チオレドキシン、ビタミンC、ビタミンEなど、ROSの消去系酵素としては、スーパーオキシドジスムターゼ、カタラーゼ、グルタチオンペルオキシダーゼ(GPx)などがある。GSHは肝に高濃度(mMレベル)で存在する物質であり、親電子物質に電子を与えて安定化する。また、GPxは、GSHを用いて過酸化水素を水と酸素に分解したり、過酸化脂質を還元したりして無毒化する。このようにGSHは、抗酸化物質として様々な役割を担っており、実際にウイルス性の肝疾患などでは炎症や線維化の進行、発がんなどに伴い、肝臓内および血中のGSHが減少することが報告されている⁸⁾。

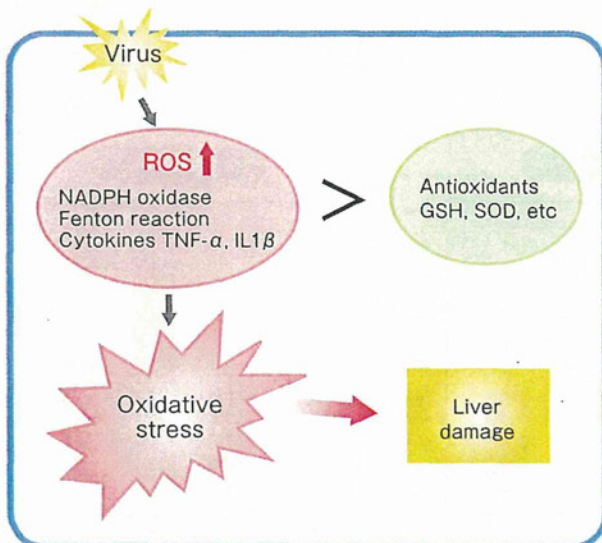
今回筆者らが見出した γ -グルタミルジペプチド

類は、グルタチオンの生合成量を示すマーカーであった。図4で示したように、肝機能マーカーであるASTとALTは、B型とC型肝炎ウイルス持続感染者であるAHBとCNALTでは健康成人と同等の値を示すが、 γ -グルタミルジペプチド類は高値を示した。HCV感染者で γ -グルタミルジペプチド類の値を比較するとCNALT>CHC>CIR>HCCであり、疾患の進行に伴い γ -グルタミルジペプチド類の値は減少した。このことはGSHの生合成量が疾患の進行とともに減少していることを示唆する。

ウイルス感染によって好中球やマクロファージのNADPHオキシダーゼやキサンチンオキシダーゼなどによってROSが産生されることが知られている。しかしCNALTでは γ -グルタミルジペプチド類は高地であり、GSHが十分に生合成されてROSを消去しているため明らかな症状が出ないのではないと思われる。しかしCHC、CIR、HCCとGSHの生合成量が減少するにつれ、生体の抗酸化システムでは消去できないROSが産生され、酸化ストレスが増幅して疾患が進行するのかもしれない(図10)。非アルコール性脂肪肝疾患でも γ -グルタミルジペプチド類の値は、SS>NASHであり、CIRの値はNASHよりもさらに低値を示した(図9)。この結果はC型肝炎ウイルスの肝疾患と同様に、疾患の進行に伴ってGSHの合成量が減少していることを示唆した。

疾患の進行とともに γ -グルタミルジペプチド類の値が減少する傾向は、GSHの生合成量が減少することを示す。GSHの生合成量が減少したことが原因で酸化ストレスが増大することによって疾患が進行していると解釈するか、あるいは反対に、肝機能が低下することによってGSHの合成量が低下した結果を γ -グルタミルジペプチド類の値が反映したものであるかは明らかではない。今度の検討課題である。

図10 ウイルス性肝疾患の発症機序



おわりに

筆者らが発見した γ -グルタミルジペプチド類は、GSHの生合成を示すマーカーであり血中の1個から数個の γ -グルタミルジペプチドあるいはメチオニンスルフォキンドやAST、ALTの値と組み合わせることで、ウイルス性、薬剤性、非アルコール性などの肝疾患患者の種類と進行度を高い精度でスクリーニングできることがわかった。またGSHの生合成量がそれぞれの疾患によって異なっており、GSHの生合成量が肝疾患の発症、進行などに重要な影響を与えている可能性を示した。今後さらに多くの検体を測定して、本法による肝疾患スクリーニング法の有用性を検証したい。

〈文献〉

- 1) Soga T, Ohashi Y, Ueno Y et al : Quantitative Metabolome Analysis Using Capillary Electrophoresis Mass Spectrometry. *J Proteome Res* 2 : 488-494, 2003.
- 2) Soga T, Baran R, Suematsu M et al : Differential Metabolomics Reveals Ophthalmic Acid As An Oxidative Stress Biomarker Indicating Hepatic Glutathione Consumption. *J Biol Chem* 281 : 16768-16776, 2006.
- 3) Soga T, Sugimoto M, Honma M et al : Serum Metabolomics Reveals γ -glutamyl Dipeptides as Biomarkers for Differentiation among Different Forms of Liver Disease. *J Hepatol*, in press.
- 4) Kaneto H, Xu G, Song KH et al : Activation of the hexosamine pathway leads to deterioration of pancreatic beta-cell function through the induction of oxidative stress. *J Biol Chem* 276 : 31099-31104, 2001.
- 5) Babior BM : Phagocytes and oxidative stress. *Am J Med* 109 : 33-44, 2000.
- 6) Griffith OW, Meister A : Potent and specific inhibition of glutathione synthesis by buthionine sulfoximine(S-n-butyl homocysteine sulfoximine). *J Biol Chem* 254 : 7558-7560, 1979.
- 7) Zalups RK, Lash LH : Depletion of glutathione in the kidney and the renal disposition of administered inorganic mercury. *Drug Metab Dispos* 25 : 516-523, 1997.
- 8) Tanyalcin T, Taskiran D, Topalak O et al : The effects of chronic hepatitis C and B virus infections on liver reduced and oxidized glutathione concentrations. *Hepatol Res* 18 : 104-109, 2000.

Metabolic Profiling to Identify Potential Serum Biomarkers for Gastric Ulceration Induced by Nonsteroid Anti-Inflammatory Drugs

Kenichiro Takeuchi,^{*,†} Maki Ohishi,[‡] Sana Ota,[‡] Kenichi Suzumura,[§] Hitoshi Naraoka,[†] Takeji Ohata,[†] Jiro Seki,[†] Youichi Miyamae,[†] Masashi Honma,^{||} and Tomoyoshi Soga[‡]

[†]Drug Safety Research Laboratories, Astellas Pharma Inc., 1-6 Kashima 2-chome, Yodogawa-ku, Osaka 532-8514, Japan

[‡]Institute for Advanced Bioscience, Keio University, 246-2 Mizukami, Kakuganji, Tsuruoka, Yamagata 997-0052, Japan

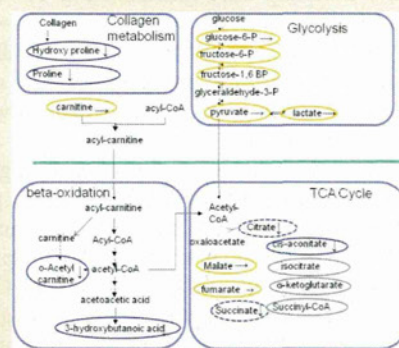
[§]Analysis and Pharmacokinetics Research Laboratories, Astellas Pharma Inc., 21, Miyukigaoka, Tsukuba-shi, Ibaraki 532-8514, Japan

^{||}Department of Pharmacy, The University of Tokyo Hospital, 7-3-1 Hongo, Bunkyo-ku, Tokyo 113-8655, Japan

Supporting Information

ABSTRACT: Nonsteroid anti-inflammatory drugs (NSAIDs) are among the most frequently prescribed drugs currently available. The most frequently reported serious side effects associated with NSAIDs are gastric mucosal ulceration and gastric hemorrhage. Presently, these side effects are only detectable by endoscopy, however, and no biomarkers have yet been identified. The ability to identify serum biomarkers would likely improve the safety of NSAID use. In this study we performed capillary electrophoresis-mass spectrometry (CE-MS)-based metabolomic profiling in stomach extract and serum from rats administered NSAIDs. Results showed drug-induced decreases in levels of citrate, *cis*-aconitate, succinate, 3-hydroxy butanoic acid, *o*-acetyl carnitine, proline, and hydroxyproline. We consider that these changes are due to NSAID-induced depression of mitochondrial function and activation of collagenase by lesions in the stomach. In addition, four of these changes in metabolite levels in the stomach were significantly correlated with changes in the serum. While further study is needed to clarify the mechanism of change in the level of these biomarkers, limitation of indications, and extrapolation to humans, these new serum biomarker candidates of gastric injury may be useful in the monitoring of NSAID-induced tissue damage.

KEYWORDS: metabolomics, capillary electrophoresis-mass spectrometry, gastric injury, nonsteroid anti-inflammatory drugs, diagnostic marker candidate



INTRODUCTION

Nonsteroid anti-inflammatory drugs (NSAIDs) are among the most frequently prescribed drugs available¹ and are commonly used to treat rheumatoid arthritis, osteoarthritis, acute pain, and fever.² The most frequently reported serious side effects associated with NSAIDs are gastric mucosal ulceration and gastric hemorrhage, with NSAID users having an approximately three times greater relative risk of serious adverse gastrointestinal events than nonusers.³ Some 15–30% of chronic NSAID users suffer from gastrointestinal ulceration and bleeding,⁴ and given that NSAIDs may mask the pain associated with gastric ulceration, patients may delay seeking medical attention, which can subsequently delay ulcer healing.⁵ Presently, gastric ulceration and hemorrhage are only detectable by endoscopy,¹ and there is an unmet medical need to identify a noninvasive means of assessing gastric injury associated with the use of NSAIDs.

Several mechanisms to explain the gastric ulceration associated with NSAID use have been suggested, including increased permeability of the stomach,⁶ inhibition of prostaglandin synthesis, mitochondria dysfunction,⁷ or any combination of these. While details of the mechanism of gastric ulceration remain to be elucidated, a number of treatment strategies to minimize the

gastrointestinal side effects of NSAID have been employed, including coadministration with proton pump inhibitors⁸ or H₂ antagonists.⁹

“Metabolomics” is a rapidly evolving technology based on highly sensitive analytical methods which are used to comprehensively analyze endogenous metabolites in samples collected from both affected patients and control subjects. Comparing concentrations of endogenous metabolites between patients and controls can help identify metabolites or metabolic pathways that may function in the pathogenesis of the disease or injury in question. Several analytical methods have been used to analyze metabolites, including mass spectrometry (MS) with gas chromatography (GC-MS),¹⁰ liquid chromatography (LC-MS),¹¹ or capillary electrophoresis (CE-MS)¹² and nuclear magnetic resonance (NMR) spectrometry.¹³ CE-MS has emerged as a powerful tool for the simultaneous analysis of endogenous metabolites in serum, urine, and organ extracts, thanks to its rapid analysis and efficient resolution (CE) with high selectivity and sensitivity (MS).¹⁴ Quantitative data for a number of metabolites at various time points and in different organs or matrices can be used to identify new biomarkers for

Received: November 6, 2012

Published: January 21, 2013

drug-induced adverse reactions, and the efficacy of this approach was demonstrated by the discovery of a plasma biomarker of acetaminophen-induced acute hepatitis in mice.^{15,16}

Here, we applied a shotgun approach based on CE-time-of-flight (TOF)-MS profiles of endogenous metabolites to identify new biomarkers of NSAID-induced gastric injury in stomach tissue extracts from rats. We then determined the correlation of concentrations of these new biomarkers in tissue extracts with that of serum concentrations.

■ EXPERIMENTAL SECTION

Study Design

Four week old male Sprague–Dawley (SD) rats (body weight: 65–85 g) obtained from Charles River Japan (Yokohama, Japan) were housed individually in stainless-steel wire mesh cages and allowed free access to a pellet diet (EC-2, Clea Japan, Inc., Tokyo, Japan) and filtered tap water (containing 2 ± 1 ppm free chlorine adjusted with sodium hypochlorite). Room temperature and relative humidity were maintained at 19–25 °C and 30–70% with 15 air changes/h and a 12 h light–dark cycle (lighted 7:00 a.m. to 7:00 p.m.). The animals were allowed to acclimatize for 1 week prior to entry into the study, and age and weight at the start of the study were recorded (age: 5 weeks; body weight: 120–140 g).

A total of 60 animals ($n = 12$ animals per group) were assigned to a control group (0.5% methylcellulose, p.o.) or one of four treatment groups: single dose aspirin (Nacalai Tesque, Kyoto, Japan) at 3 mg/kg, p.o., single dose aspirin at 300 mg/kg, p.o., single dose ibuprofen (Wako Pure Chemical Industries, Ltd., Kyoto, Japan) at 8 mg/kg, p.o., or single dose ibuprofen at 800 mg/kg, p.o. The doses used in this study were based on preliminary results (data not shown) in which the higher doses of the two compounds (300 mg/kg aspirin and 800 mg/kg ibuprofen) were demonstrated to induce gastric lesions, while the lower doses (3 mg/kg aspirin and 8 mg/kg ibuprofen) were found not to induce lesions.

All experiments were carried out at Shin Nippon Biomedical Laboratories, Ltd. (Tokyo, Japan). This study was approved by the Institutional Animal Care and Use Committee of Shin Nippon Biomedical Laboratories, Ltd., and the Animal Ethical Committee of Astellas Pharma Inc. (Tokyo, Japan).

Sample Collection

Rats were anesthetized (sodium pentobarbital 32.4 mg/kg, i.p.) and exsanguinated via the abdominal aorta at 1, 5, or 24 h after dosing. Serum was collected by allowing the blood to clot at room temperature for 20 min followed by centrifugation at $1710 \times g$. Immediately after exsanguination, the stomach was collected and incised along the greater curvature. The tissue was then assessed macroscopically, and the interior of the stomach was photographed. The dimensions of observed gastric ulcers were determined using analySIS software (Olympus Soft Imaging Solutions GmbH, Münster, Germany). After being photographed, the stomachs were weighed, frozen in liquid nitrogen, and stored at -70 °C until sample preparation.

Sample Preparation for CE–MS

For tissue preparation, frozen stomach tissue was plunged into ice-chilled methanol (1 mL) containing internal standards (10 μ M each of methionine sulfone [Wako, Osaka, Japan], D-camphor-10-sulfonic acid [CAS; Wako], and 2-(*n*-morpholino)-ethanesulfonic acid [MES; Dojindo, Kumamoto, Japan]), and then water and chloroform were added. After the homogenized

tissue was mixed thoroughly, the solution was centrifuged at $4600 \times g$ for 20 min at 4 °C. A 500 μ L aliquot of the upper aqueous layer was then centrifugally filtered through a Millipore 5 kDa cutoff filter to remove proteins, and the filtrate was lyophilized and dissolved in 50 μ L of Milli-Q water containing reference compounds (200 μ M 3-aminopyrrolidine and 200 μ M trimesate).

For serum preparation, a 50 μ L aliquot of serum was added to 450 μ L of methanol containing internal standards (20 μ M each of methionine sulfone, CAS, and MES) and mixed well. Deionized water (200 μ L) and 500 μ L chloroform were then added, and the solution was centrifuged at $4600 \times g$ for 8 min at 4 °C. The upper aqueous layer (approximately 800 μ L) was centrifugally filtered through a Millipore 5 kDa cutoff filter to remove proteins, and the filtrate was lyophilized and dissolved in 50 μ L of Milli-Q water containing reference compounds (200 μ M 3-aminopyrrolidine and 200 μ M trimesate).

Metabolite Standards

All chemical standards were obtained from common commercial sources. Standards were dissolved in Milli-Q water, 0.1 M HCl, or 0.1 M NaOH to obtain 10 or 100 mM stock solutions. Working standard mixtures were prepared by diluting stock solutions with Milli-Q water just prior to injection into the CE–TOF-MS system. All chemicals used as standards were of analytical or reagent grade.

Instrumentation

All CE–TOF-MS experiments were performed using an Agilent CE capillary electrophoresis system (Agilent Technologies, Waldbronn, Germany), an Agilent G3250AA LC–MSD TOFMS system (Agilent Technologies, Palo Alto, CA, U.S.A.), an Agilent 1100 isocratic HPLC pump, an Agilent G1603A CE–MS adapter kit, and an Agilent G1607A CE–Electro Spray Ionization (ESI)–MS sprayer kit. System control and data acquisition were done using the Agilent G2201AA ChemStation software for CE and Analyst QS for TOF-MS.

CE–TOF-MS Conditions for Cationic Metabolite analysis

Separations were carried out in a fused silica capillary (50 μ m inner diameter \times 100 cm total length) filled with 1 M formic acid as the electrolyte.¹⁷ Approximately 3 nL of sample solution was injected at 50 mbar for 3 s, followed by application of 30 kV. Capillary temperature was maintained at 20 °C, and the sample tray was cooled below 5 °C. Methanol/water (50% [v/v]) containing 0.1 μ M hexakis(2,2-difluoroethoxy)phosphazene was delivered as the sheath liquid at a flow rate of 10 μ L/min. ESI–TOF-MS was operated in the positive ion mode, and capillary voltage was set at 4 kV. A flow rate of heated dry nitrogen gas (heater temperature, 300 °C) was maintained at 10 psi. In TOF-MS, the fragmenter, skimmer, and Oct RFV voltage were set at 75, 50, and 125 V, respectively. Automatic recalibration of each acquired spectrum was achieved using the masses of reference standards ($[^{13}\text{C}$ isotopic ion of a protonated methanol dimer (2MeOH + H)]⁺, m/z 66.0632) and ([hexakis(2,2-difluoroethoxy)phosphazene + H]⁺, m/z 622.0290). Exact mass data were acquired at a rate of 1.5 spectra/s over a 50–1000 m/z range. Total run time, including capillary preconditioning, was 45 min.

CE–TOF-MS Conditions for Anionic Metabolite Analysis

A commercially available COSMO (+) capillary (50 μ m inner diameter \times 100 cm total length; Nacalai Tesque, Kyoto, Japan),¹⁸ chemically coated with a cationic polymer, was used as the separation capillary.¹⁹ A 50 mM ammonium acetate solution (pH 8.5) was used as electrolyte solution for CE separation.

Approximately 30 nL of sample solution was injected at 50 mbar for 30 s, followed by application of -30 kV. Ammonium acetate (5 mM) in 50% methanol/water (v/v) containing $0.1 \mu\text{M}$ hexakis(2,2-difluoroethoxy) phosphazene was delivered as the sheath liquid at a flow rate of $10 \mu\text{L}/\text{min}$. ESI-TOF-MS was conducted in the negative ion mode, with the capillary voltage set at 3.5 kV. For TOF-MS, the fragmenter, skimmer, and Oct

RFV voltage were set at 100, 50, and 200 V, respectively. Automatic recalibration of each acquired spectrum was performed using reference masses of reference standards ($[^{13}\text{C}$ isotopic ion of deprotonated acetic acid dimer $(2\text{CH}_3\text{COOH-H})^-$, m/z 120.03841), and ($[\text{hexakis} + \text{deprotonated acetic acid } (\text{CH}_3\text{COOH-H})^-]$, m/z 680.03554). Other conditions were identical to those previously reported.¹⁹ Total run time, including capillary preconditioning, was 40 min.

Table 1. Severity of Gastric Ulceration Evaluated as Area of Ulceration^a

	control	aspirin		ibuprofen	
		3 mg/kg	300 mg/kg	8 mg/kg	800 mg/kg
1 h	ND (0/4)	ND (0/4)	ND (0/4)	ND (0/4)	ND (0/4)
5 h	ND (0/4)	ND (0/4)	2.48 ± 1.14 (4/4)	ND (0/4)	18.08 ± 18.72 (4/4)
24 h	ND (0/4)	ND (0/4)	0.08 ± 0.15 (1/4)	ND (0/4)	3.76 ± 4.33 (4/4)

^aData are expressed as mean + SD of the area of ulceration (mm^2). Values in parentheses are the incidence rate of animals with gastric ulceration. ND: not detected.

Data Processing for Generation of the Metabolome Differential Display

To reduce data analysis time, raw data sets were preprocessed by binning the data along the m/z axis to $0.02 m/z$ resolution, subtracting the baseline from each electropherogram by robust nonlinear fitting of the data to a seventh-order polynomial, and removing the noise from each electropherogram by leveling to 0 all signal intensity values that fell within 5 SD of the signal intensities from 1 to 4 min. The resulting data sets were then further binned to 1 m/z unit resolution along the m/z axis. A set of peaks was selected from each data set using a modified Douglas-Peucker algorithm, with alignment of data sets along the migration time axis as described in the text. Annotation tables for both cation and anion modes were generated based on the

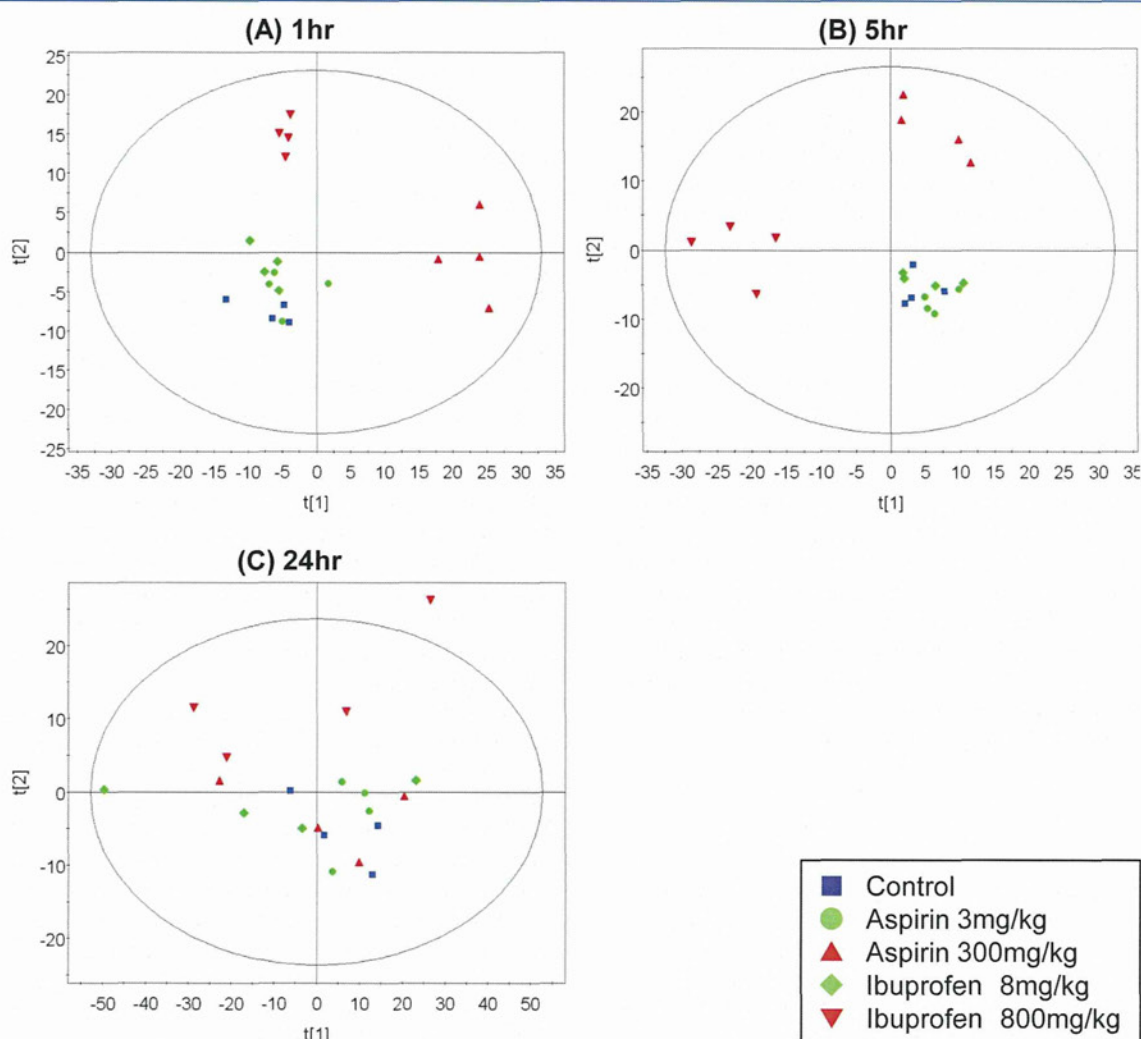


Figure 1. PCA score plots obtained from CE-MS data of stomach at 1 h (A), 5 h (B), and 24 h (C) after dosing. PCA score plot indicating discrimination between control and high-dose aspirin (300 mg/kg) or ibuprofen (800 mg/kg) at 1 and 5 h after dosing in two-dimensional PCA scores plot. This separation at 24 h after dosing was not as clear as that at 1 or 5 h postdose. Animals from the low-dose aspirin (3 mg/kg) and ibuprofen (8 mg/kg) groups showed almost the same pattern as the control group throughout the observation period.

Table 2. Measured Levels of Metabolites in Stomach between Groups at 1, 5, and 24 h after Administration^a

metabolite	time point	control	aspirin		ibuprofen	
			3 mg/kg	300 mg/kg	8 mg/kg	800 mg/kg
citrate	1 h	194 ± 21	202 ± 23	120 ± 25 (**)	202 ± 26	135 ± 39 (*)
	5 h	190 ± 18	187 ± 33	120 ± 8 (**)	172 ± 23	124 ± 19 (**)
	24 h	269 ± 75	203 ± 42	213 ± 50	175 ± 60	169 ± 52
<i>cis</i> -aconitate	1 h	4.7 ± 0.3	4.4 ± 0.5	2.8 ± 0.7	4.6 ± 0.6	3.6 ± 1.0
	5 h	5.4 ± 0.6	4.6 ± 1.0	3.1 ± 0.4 (**)	4.1 ± 1.0 (*)	3.1 ± 0.9 (**)
	24 h	7.7 ± 2.0	5.6 ± 0.7	5.7 ± 1.0	4.9 ± 1.6 (*)	3.7 ± 1.1 (**)
succinate	1 h	235 ± 34	252 ± 30	227 ± 28	229 ± 29	139 ± 27 (**)
	5 h	220 ± 7	231 ± 14	195 ± 8 (*)	205 ± 11	155 ± 11 (**)
	24 h	349 ± 60	323 ± 44	295 ± 80	270 ± 110	278 ± 87
<i>o</i> -acetyl carnitine	1 h	201 ± 14	196 ± 9	150 ± 20 (*)	206 ± 36	149 ± 29 (*)
	5 h	205 ± 9	198 ± 39	128 ± 13 (**)	164 ± 12	131 ± 25 (**)
	24 h	237 ± 41	237 ± 33	193 ± 41	195 ± 75	145 ± 39
3-hydroxybutanoic acid	1 h	565 ± 141	575 ± 110	285 ± 67 (*)	445 ± 234	188 ± 60 (**)
	5 h	690 ± 326	610 ± 211	206 ± 40 (*)	394 ± 130	404 ± 134
	24 h	596 ± 298	397 ± 217	317 ± 227	326 ± 206	175 ± 70 (*)
proline	1 h	339 ± 23	325 ± 28	274 ± 24 (**)	329 ± 25	317 ± 18
	5 h	274 ± 23	303 ± 24	247 ± 10	292 ± 22	233 ± 17 (*)
	24 h	434 ± 78	433 ± 35	428 ± 131	367 ± 134	385 ± 98
hydroxyproline	1 h	158 ± 14	130 ± 10 (*)	113 ± 8 (**)	128 ± 19 (*)	130 ± 10 (*)
	5 h	118 ± 23	128 ± 13	65 ± 11 (**)	118 ± 24	89 ± 21 (*)
	24 h	171 ± 46	154 ± 28	145 ± 36	122 ± 37	100 ± 26

^aMean concentration (nmol/g tissue) and standard deviation. Asterisks indicate statistically significant differences: **, $p < 0.01$; *, $p < 0.05$.

results of CE–TOF–MS analysis of standard compounds. The annotation labels were aligned to the actual data sets in a similar fashion. Arithmetic operations were applied to whole data sets on a data point-by-data point basis to highlight differences of interest. Averaging the data sets within each group allowed visualization of absolute (difference between the corresponding intensities from the averaged data sets) and relative (absolute difference divided by the larger of the two corresponding intensities) differences.

The concentrations of endogenous metabolites were imported into SIMCA-P+, version 12.0 (Umetrics, AB, Umea, Sweden). Principal components analysis (PCA) and orthogonal partial least-squares (O-PLS) were applied to get an overview of systematic variations among all observations and to identify endogenous metabolites correlated with gastric damage, respectively. To compare compound levels between groups, ANOVA and Dunnett's test were performed using GraphPad Prism, version 5.03 (GraphPad Software, San Diego, CA, U.S.A.). To analyze the correlation between the concentration of each metabolite in stomach and serum, Pearson's product-moment correlation coefficient was calculated and statistically analyzed using GraphPad Prism, version 5.03 (GraphPad Software).

RESULTS

Gastric Ulceration

The severity of gastric ulceration was presented as the ulcerative area for each group tested at one of three time points following drug administration (Table 1). No gastric ulceration was noted in control animals at any observation point following oral administration of 0.5% methylcellulose or in any animals administered either test compound at the low dose. In addition, no gastric ulceration was noted 1 h postdose in animals administered high-dose aspirin (300 mg/kg) or ibuprofen (800 mg/kg). However, by 5 h postadministration, both of the high-dose NSAID groups showed gastric ulceration, although the areas of ulceration were reduced by

97% and 79% at 24 h postdose in the aspirin and ibuprofen groups, respectively.

Metabolomic Analysis of Stomach Tissue Extracts

A total of 580 peaks were identified and quantified with metabolite standards matching the closest m/z value and normalized migration time for further statistical comparison and interpretations using the CE–TOF–MS system. (Supporting Information, Table 1) Although additional unnamed analytes were observed, we discuss only identified metabolites in the present study. As presented in Figure 1, clear separation was detected between control and high-dose aspirin (300 mg/kg) or ibuprofen (800 mg/kg) at 1 and 5 h after dosing in the two-dimensional PCA scores plot. This separation at 24 h after dosing was not as clear as at 1 or 5 h postdosing. The animals in the low-dose aspirin (3 mg/kg) and ibuprofen (8 mg/kg) groups showed almost the same pattern as that in the control group throughout the observation period. These findings suggest that these separations reflected the induction and recovery of gastric ulceration as observed in the pathological study.

Statistical analysis of quantitative differences between groups showed decreases in the levels of citrate, *cis*-aconitate, succinate, *o*-acetylcarnitine, and 3-hydroxybutanoic acid. In addition to these, decreases were also observed in proline and hydroxyproline levels in the stomach tissue extracts (Table 2 and Supporting Information, Figure 1). The selected CE–TOF–MS ion electropherograms of these metabolites are shown in Figure 2.

We superimposed metabolite concentrations changes from stomach tissue extracts on metabolic pathway maps, including those for the tricarboxylic acid cycle (TCA) cycle, β -oxidation, and glycolysis. The concentration of some metabolites in these pathways was too low for accurate detection by CE–TOF–MS, and changes in them could not be detected. While we noted suppression of the TCA cycle and β -oxidation on administration of NSAIDs, glycolysis—the upper stream of the TCA cycle—was unaffected (Figure 3).

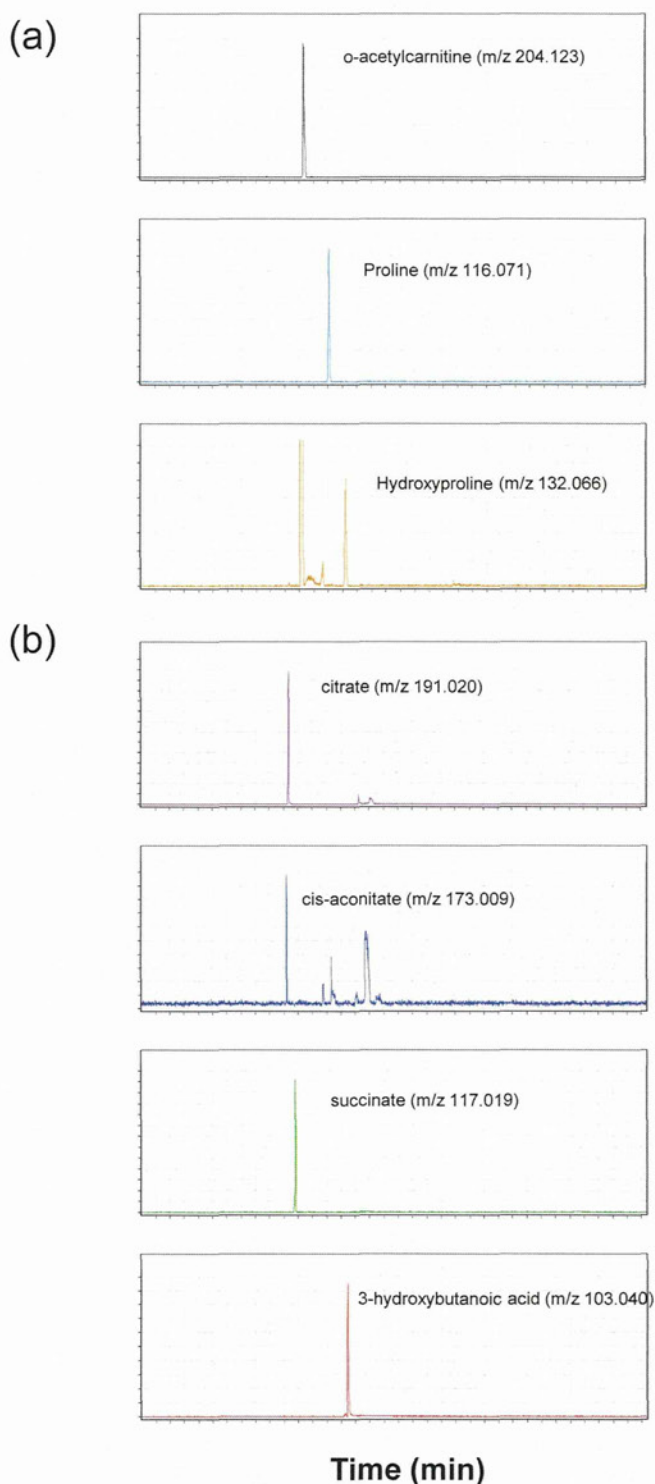


Figure 2. Selected CE-TOF-MS ion electropherograms for the stomach tissue of cationic (a) and anionic (b) metabolites.

Metabolomic Analysis of Serum

CE-TOF-MS was used to identify and quantify 580 peaks with metabolite standards matching the closest m/z value and normalized migration time for further statistical comparison and interpretation (Supporting Information, Table 1). Although additional unnamed analytes were observed, we discussed only identified metabolites in the present study. As presented in Figure 4, clear separation was detected between control and

high-dose aspirin (300 mg/kg) or ibuprofen (800 mg/kg) at 1 and 5 h after dosing in the two-dimensional PCA scores plot. Findings for quantified serum levels of these metabolites in each group at 1, 5, and 24 h after administration are presented in Table 3 and Supporting Information, Figure 2. Decreases in serum levels of *cis*-aconitate, succinate, *o*-acetyl carnitine, 3-hydroxybutanoic acid proline, and hydroxyproline levels were observed, with similar changes noted in stomach tissue extracts. In contrast, no changes were noted in serum citrate concentration.

We also assessed the correlation between concentrations of each metabolite in stomach tissue extracts and serum (Table 3). Results showed that the serum levels of each metabolite except succinate were significantly correlated with the concentrations in stomach tissue extracts.

DISCUSSION

Here, to identify candidate biomarkers of NSAID-induced gastric injury, we applied the metabolome differential display method based on CE-MS to a rat model of gastric ulcer induced by NSAIDs. We identified four new candidate biomarkers in the stomach which reflect this ulceration and can be detected by changes in their serum levels. Given that no biomarkers of NSAID-induced gastric ulceration in serum have yet been identified, these findings should be useful for monitoring NSAID-induced tissue damage in serum. A monitoring method using these biomarker candidates is expected to replace the current invasive practice of endoscopy.

NSAIDs, such as aspirin and ibuprofen, are among the most frequently prescribed drugs available and are commonly prescribed as analgesic, antipyretic, and anti-inflammatory drugs. Despite their widespread use, however, all NSAIDs are associated with an increased risk of gastric mucosal ulceration and hemorrhage. Given that such adverse effects are often asymptomatic and detectable only by gastric endoscopy, gastric injury associated with NSAID use can progress to life-threatening gastric ulceration and bleeding prior to detection.¹

Administration of NSAIDs at doses that induced gastric injury in rats was associated with decreases in levels of citrate, *cis*-aconitate, succinate, *o*-acetyl carnitine, 3-hydroxy butanoic acid, proline, and hydroxyproline in stomach tissue extracts compared with tissue extracts collected from vehicle-treated control animals. Plotting these metabolite changes on metabolic pathway maps demonstrated that two events were associated with NSAID-induced gastric injury: (1) hyperactivity of collagenase in the stomach and (2) decreases in levels of citrate, *cis*-aconitate, and succinate as indications of altered TCA cycle activity, and in levels of *o*-acetyl carnitine and 3-hydroxybutanoic acid as indications of an altered acyl-carnitine pathway, both of which are mitochondrial pathways and suggest depressed mitochondrial function.

NSAIDs have been reported to induce the opening of mitochondrial permeability transition pores,⁷ which in turn induces the uncoupling of oxidative phosphorylation, increases resting state respiration, and disrupts mitochondrial transmembrane potential.^{20–25} These changes in mitochondrial energy production induced by NSAIDs are thought to play an important role in the induction of tissue damage.²⁶ In the present study, levels of citrate, *cis*-aconitate, and succinate, which are intermediates of the TCA cycle, were all decreased in stomach tissue, suggesting that the TCA cycle was inhibited by NSAIDs. However, we noted no significant changes in levels of other TCA intermediates, such as fumarate or malate, suggesting that these compounds may represent entry points for amino acid metabolism. Further, NSAID administration was associated with

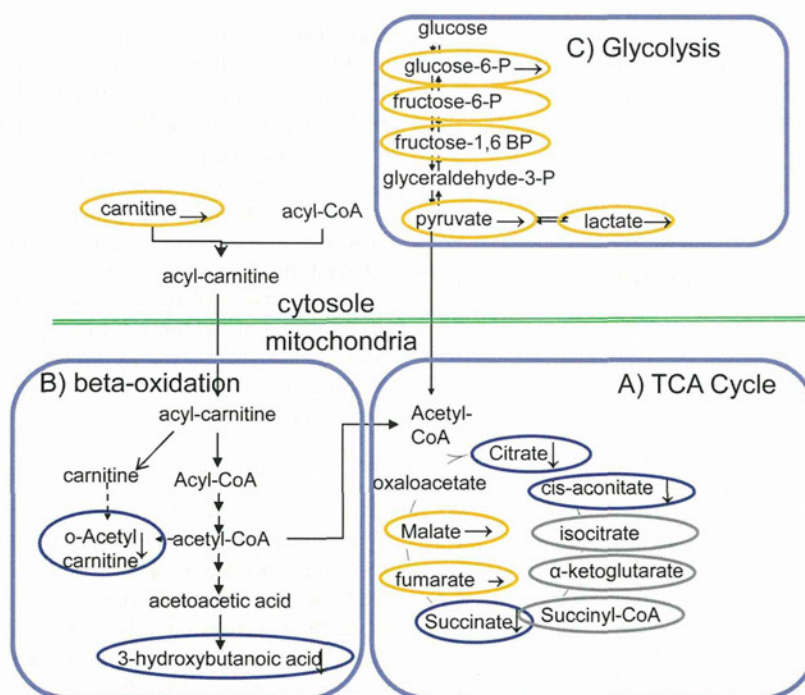


Figure 3. Observed metabolite changes in levels of stomach metabolites by a high dose of aspirin or ibuprofen mapped onto pathways. The metabolites are involved in the TCA cycle (A), β -oxidization (B), and glycolysis (C). Data were obtained by simultaneous analysis of altered levels of metabolites using CE–TOF-MS. The metabolites indicated by a blue sphere were significantly decreased by a high dose of NSAIDs. The metabolites indicated by a yellow sphere were not changed by a high dose of NSAIDs. Changes in metabolites indicated by a gray sphere could not be detected because concentrations were below detection limits.

Table 3. Measured Levels of Metabolites in Serum between Groups at 1, 5, and 24 h after Administration^a

metabolite	time point	control	aspirin		ibuprofen		correlation
			3 mg/kg	300 mg/kg	8 mg/kg	800 mg/kg	
citrate	1 h	112 ± 5	99 ± 10	99 ± 14	112 ± 13	113 ± 8	$p < 0.01$
	5 h	116 ± 9	106 ± 10	97 ± 13	103 ± 6	100 ± 10	
	24 h	106 ± 7	96 ± 6	94 ± 18	96 ± 5	84 ± 3	
cis-aconitate	1 h	5.3 ± 0.2	5.0 ± 0.8	4.7 ± 0.5	5.4 ± 0.5	5.7 ± 0.6	$p < 0.01$
	5 h	5.8 ± 0.6	5.6 ± 0.6	4.2 ± 0.3 (**)	5.3 ± 0.5	5.1 ± 0.4	
	24 h	5.8 ± 0.9	5.4 ± 0.1	5.0 ± 0.8	5.5 ± 0.1	5.2 ± 0.3	
succinate	1 h	20 ± 2	19 ± 3	18 ± 1	18 ± 1	18 ± 2	NS
	5 h	22 ± 2	20 ± 1 (*)	24 ± 1	20 ± 1	19 ± 0 (**)	
	24 h	19 ± 1	19 ± 2	17 ± 1	18 ± 2	21 ± 3	
o-acetyl carnitine	1 h	11.4 ± 1.5	11.6 ± 1.6	11.8 ± 4.4	12.4 ± 2.1	8.8 ± 1.4	$p < 0.01$
	5 h	15.6 ± 3.9	14.3 ± 1.6	8.7 ± 1.0 (**)	9.8 ± 1.3 (*)	7.3 ± 2.6 (**)	
	24 h	15.1 ± 3.6	17.0 ± 2.6	15.1 ± 0.7	20.6 ± 8.9	8.0 ± 2.4	
3-hydroxybutanoic acid	1 h	1299 ± 241	1253 ± 130	579 ± 101 (**)	983 ± 343	466 ± 152 (*)	$p < 0.01$
	5 h	1515 ± 731	1260 ± 261	320 ± 102 (**)	880 ± 203 (*)	660 ± 213 (**)	
	24 h	971 ± 477	725 ± 235	501 ± 299	699 ± 293	311 ± 128 (*)	
proline	1 h	160 ± 18	157 ± 19	116 ± 18 (**)	137 ± 13	135 ± 14	$p < 0.01$
	5 h	150 ± 14	141 ± 10	118 ± 14 (*)	149 ± 16	104 ± 16 (**)	
	24 h	138 ± 5	153 ± 13	139 ± 26	140 ± 10	127 ± 20	
hydroxyproline	1 h	57 ± 5	51 ± 5	40 ± 8 (**)	50 ± 3	51 ± 3	$p < 0.01$
	5 h	52 ± 6	53 ± 4	28 ± 4 (**)	52 ± 6	41 ± 5 (*)	
	24 h	47 ± 5	46 ± 10	38 ± 10	43 ± 5	30 ± 8 (*)	

^aMean concentration (nmol/mL) and SD. Asterisks indicate statistically significant differences. **, $p < 0.01$; *, $p < 0.05$. NS: not significant.

a decrease in 3-hydroxy butanoic acid levels from stomach tissue extracts. Given that 3-hydroxy butanoic acid is a final product and marker of fatty acid β -oxidation, decreased levels of this compound may indicate that NSAIDs also suppressed fatty acid β -oxidation.

In contrast, no changes were observed in levels of intermediates of glycolysis. Under normal conditions, pyruvate, a final

product of glycolysis, is converted to acetyl-CoA, which is further incorporated into the TCA cycle for energy production. Glycolysis occurs in the cytoplasm, while the TCA cycle and fatty acid β -oxidation occur in mitochondria. The observed suppression of the TCA cycle and fatty β -oxidation with no noticeable effect on glycolysis therefore suggests an impairment of mitochondrial activity.

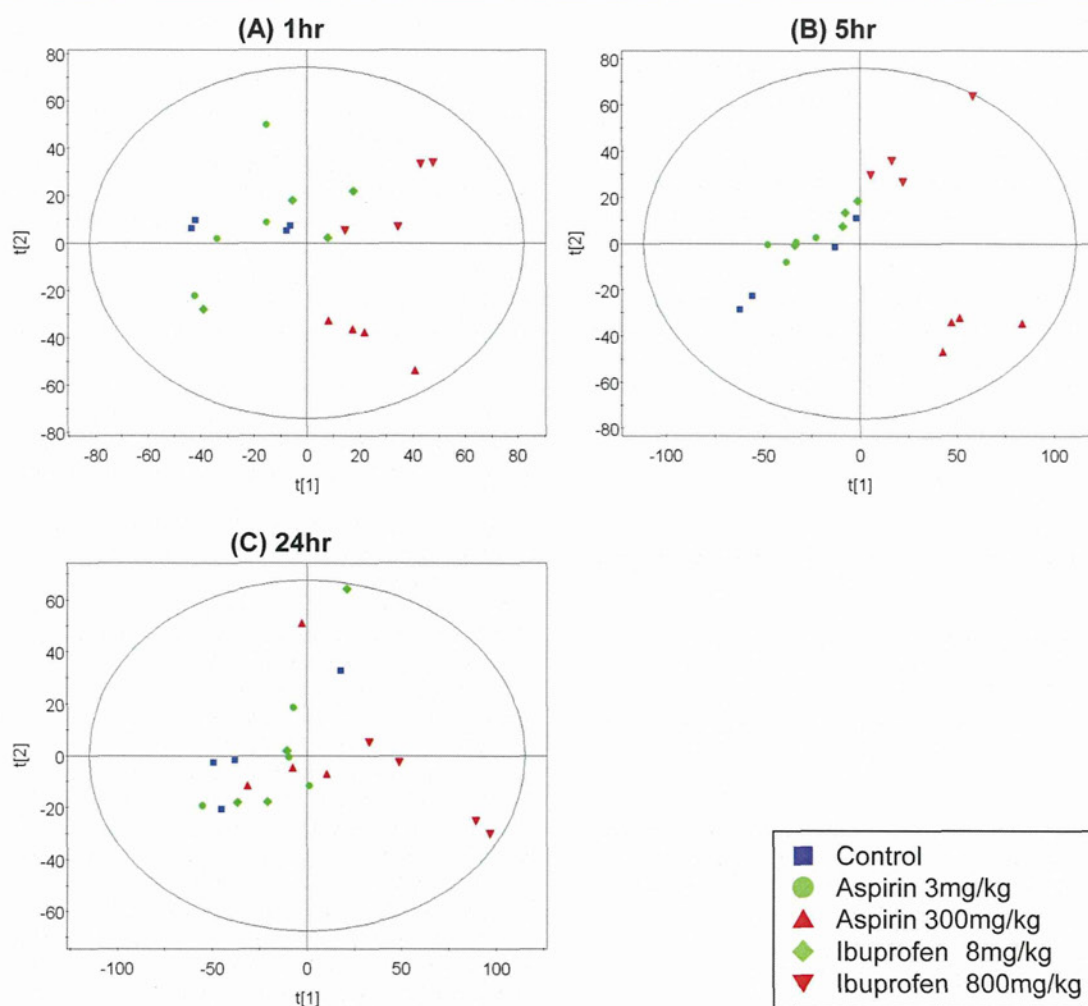


Figure 4. PCA score plots obtained from CE–MS data of serum at 1 h (A), 5 h (B), and 24 h (C) after dosing. PCA score plot indicating discrimination between the control and high-dose aspirin (300 mg/kg) or ibuprofen (800 mg/kg) groups at 1 and 5 h after dosing in two-dimensional PCA scores plot. This separation at 24 h after dosing was not as clear as that at 1 or 5 h postdose. The animals from the low-dose aspirin (3 mg/kg) or ibuprofen (8 mg/kg) groups showed almost the same pattern as the control group throughout the observation period.

Decreases in proline and hydroxyproline in stomach tissue extracts were also observed. Hydroxyproline is a modified amino acid specifically found in collagen, and proline is an amino acid which can also be found in collagen. We therefore consider that these findings are indicative of decreased collagen levels in the stomach. Indeed, previous studies have reported increased collagenase activity and a decreased amount of collagen in stomach tissue afflicted with NSAID-induced ulcers.²⁷ In the present study, levels of proline and hydroxyproline began to decline at 1 h after administration, with increasingly severe declines observed up to 5 h after administration and subsequent recovery at 24 h after. These changes were believed to parallel changes in gastric ulcer dimensions. While decreases in proline and hydroxyproline levels had already begun at 1 h after administration, no changes were observed at this point in the stomach. However, given that gastric ulcers were observed in all animals in both high-dose treatment groups by 5 h after administration, we surmised that gastric ulceration had indeed begun at 1 h after of administration, but that the ulcers were too small to detect on gross pathology. Accordingly, we consider that decreased levels of proline and hydroxyproline are more sensitive, earlier markers of gastric ulceration than gross pathology.

Once new biomarker candidates of gastric injury had been identified in the stomach tissue, we then assessed the levels of these same candidates in serum. Using this approach, we were able to identify noninvasively monitorable biomarker candidates of gastric ulceration induced by NSAIDs. The data showed that decreases in levels of *cis*-aconitate, *o*-acetyl carnitine, 3-hydroxybutanoic acid, proline, and hydroxyproline in stomach tissue extracts were significantly correlated with similar changes in the serum levels of these compounds, strongly suggesting that NSAID-induced changes in levels of these endogenous metabolites in the stomach are monitorable in the serum and accordingly making them favorable candidates for biomarkers of gastric injury in serum. In contrast, while decreases in citrate in the stomach were well correlated with those in serum, the degree of decrease was small and without statistical significance. A decrease in succinate in the serum was not correlated with that in the stomach. Further study is needed to clarify the mechanism of change in these biomarkers, limitation of indications, and extrapolation for application in humans. Nevertheless, these new biomarker candidates of gastric injury may prove useful for monitoring NSAID-induced tissue damage in place of the current invasive practice of endoscopy.

CONCLUSIONS

Serum and stomach tissue extract metabolic profiles obtained using CE-MS from rats treated with NSAIDs showed drug-induced decreases in levels of citrate, *cis*-aconitate, succinate, *o*-acetyl carnitine, 3-hydroxy butanoic acid, proline, and hydroxyproline. These changes were considered due to NSAID-induced depression of mitochondrial function and activation of collagenase by lesions in the stomach. In addition, four of these changes in metabolite levels in the stomach were significantly correlated with changes in the serum. While further study is needed to clarify the mechanism of change in these biomarkers, limitation of indications, and extrapolation to humans, these new non-invasive biomarker candidates of gastric injury might be useful in the monitoring of NSAID-induced tissue damage.

ASSOCIATED CONTENT

Supporting Information

This material is available free of charge via the Internet at <http://pubs.acs.org>.

AUTHOR INFORMATION

Corresponding Author

*E-mail: kenichiro.takeuchi@astellas.com. Telephone: +81-6-6210-7057.

Notes

The authors declare the following competing financial interest(s): This study was carried out with support from a grant from the Ministry of health, Labor and Welfare, Drug Discovery Platform Research (H20-bio-ippan-011).

ACKNOWLEDGMENTS

We are grateful to Hideaki Okatani for his technical assistance in caring for the rats and preparing samples. We also thank Dr. Marlowe Schneidkraut for his review of the manuscript and for his suggestions regarding the study. This study was carried out with support from a grant from the Ministry of health, Labor and Welfare, Drug Discovery Platform Research (H20-bio-ippan-011).

REFERENCES

- (1) Steinmeyer, J. Pharmacological basis for the therapy of pain and inflammation with nonsteroidal anti-inflammatory drugs. *Arthritis Res.* **2000**, *2* (5), 379–85.
- (2) Gabriel, S. E.; Fehring, R. A. Trends in the utilization of nonsteroidal anti-inflammatory drugs in the United States, 1986–1990. *J. Clin. Epidemiol.* **1992**, *45* (9), 1041–4.
- (3) Gabriel, S. E.; Jaakkimainen, L.; Bombardier, C. Risk for serious gastrointestinal complications related to use of nonsteroidal anti-inflammatory drugs. A meta-analysis. *Ann. Intern. Med.* **1991**, *115* (10), 787–96.
- (4) Ishihara, T.; Tanaka, K.; Tashiro, S.; Yoshida, K.; Mizushima, T. Protective effect of rebamipide against celecoxib-induced gastric mucosal cell apoptosis. *Biochem. Pharmacol.* **2010**, *79* (11), 1622–33.
- (5) Hawkey, C. J. Nonsteroidal anti-inflammatory drug gastropathy. *Gastroenterology* **2000**, *119* (2), 521–35.
- (6) Sutherland, L. R.; Verhoef, M.; Wallace, J. L.; Van Rosendaal, G.; Crutcher, R.; Meddings, J. B. A simple, non-invasive marker of gastric damage: sucrose permeability. *Lancet* **1994**, *343* (8904), 998–1000.
- (7) Szewczyk, A.; Wojtczak, L. Mitochondria as a pharmacological target. *Pharmacol. Rev.* **2002**, *54* (1), 101–27.
- (8) Richardson, P.; Hawkey, C. J.; Stack, W. A. Proton pump inhibitors. Pharmacology and rationale for use in gastrointestinal disorders. *Drugs* **1998**, *56* (3), 307–35.
- (9) Takeda, M.; Takagi, T.; Yashima, Y.; Maeno, H. Effect of a new potent H₂-blocker, 3-[[[2-(diaminomethylene)amino]-4-thiazolyl]-methyl]thio]-N₂-sulfamoyl propionamide (YM-11170), on gastric secretion, ulcer formation and weight of male accessory sex organs in rats. *Arzneimittelforschung* **1982**, *32* (7), 734–7.
- (10) Fiehn, O.; Kopka, J.; Dormann, P.; Altmann, T.; Trethewey, R. N.; Willmitzer, L. Metabolite profiling for plant functional genomics. *Nat. Biotechnol.* **2000**, *18* (11), 1157–61. (b) Schauer, N.; Semel, Y.; Roessner, U.; Gur, A.; Balbo, I.; Carrari, F.; Pleban, T.; Perez-Melis, A.; Bruedigam, C.; Kopka, J.; Willmitzer, L.; Zamir, D.; Fernie, A. R. Comprehensive metabolic profiling and phenotyping of interspecific introgression lines for tomato improvement. *Nat. Biotechnol.* **2006**, *24* (4), 447–54.
- (11) Plumb, R.; Granger, J.; Stumpf, C.; Wilson, I. D.; Evans, J. A.; Lenz, E. M. Metabonomic analysis of mouse urine by liquid-chromatography-time of flight mass spectrometry (LC-TOFMS): detection of strain, diurnal and gender differences. *Analyst* **2003**, *128* (7), 819–23.
- (12) Monton, M. R.; Soga, T. Metabolome analysis by capillary electrophoresis-mass spectrometry. *J. Chromatogr. A* **2007**, *1168* (1–2), 237–46 discussion 236.
- (13) Nicholson, J. K.; Connelly, J.; Lindon, J. C.; Holmes, E. Metabonomics: a platform for studying drug toxicity and gene function. *Nat. Rev. Drug Discovery* **2002**, *1* (2), 153–61.
- (14) Soga, T.; Ohashi, Y.; Ueno, Y.; Naraoka, H.; Tomita, M.; Nishioka, T. Quantitative metabolome analysis using capillary electrophoresis mass spectrometry. *J. Proteome Res.* **2003**, *2* (5), 488–94.
- (15) Soga, T.; Baran, R.; Suematsu, M.; Ueno, Y.; Ikeda, S.; Sakurakawa, T.; Kakazu, Y.; Ishikawa, T.; Robert, M.; Nishioka, T.; Tomita, M. Differential metabolomics reveals ophthalmic acid as an oxidative stress biomarker indicating hepatic glutathione consumption. *J. Biol. Chem.* **2006**, *281* (24), 16768–76.
- (16) Shintani, T.; Iwabuchi, T.; Soga, T.; Kato, Y.; Yamamoto, T.; Takano, N.; Hishiki, T.; Ueno, Y.; Ikeda, S.; Sakuragawa, T.; Ishikawa, K.; Goda, N.; Kitagawa, Y.; Kajimura, M.; Matsumoto, K.; Suematsu, M. Cystathionine beta-synthase as a carbon monoxide-sensitive regulator of bile excretion. *Hepatology* **2009**, *49* (1), 141–50.
- (17) Soga, T.; Heiger, D. N. Amino acid analysis by capillary electrophoresis electrospray ionization mass spectrometry. *Anal. Chem.* **2000**, *72* (6), 1236–41.
- (18) Katayama, H.; Ishihama, Y.; Asakawa, N. Stable cationic capillary coating with successive multiple ionic polymer layers for capillary electrophoresis. *Anal. Chem.* **1998**, *70* (24), 5272–7.
- (19) Soga, T.; Igarashi, K.; Ito, C.; Mizobuchi, K.; Zimmermann, H. P.; Tomita, M. Metabolomic profiling of anionic metabolites by capillary electrophoresis mass spectrometry. *Anal. Chem.* **2009**, *81* (15), 6165–74.
- (20) Petrescu, I.; Tarba, C. Uncoupling effects of diclofenac and aspirin in the perfused liver and isolated hepatic mitochondria of rat. *Biochim. Biophys. Acta* **1997**, *1318* (3), 385–94.
- (21) Moreno-Sanchez, R.; Bravo, C.; Vasquez, C.; Ayala, G.; Silveira, L. H.; Martinez-Lavin, M. Inhibition and uncoupling of oxidative phosphorylation by nonsteroidal anti-inflammatory drugs: study in mitochondria, submitochondrial particles, cells, and whole heart. *Biochem. Pharmacol.* **1999**, *57* (7), 743–52.
- (22) Mingatto, F. E.; Santos, A. C.; Uyemura, S. A.; Jordani, M. C.; Curti, C. In vitro interaction of nonsteroidal anti-inflammatory drugs on oxidative phosphorylation of rat kidney mitochondria: respiration and ATP synthesis. *Arch. Biochem. Biophys.* **1996**, *334* (2), 303–8.
- (23) Masubuchi, Y.; Yamada, S.; Horie, T. Diphenylamine as an important structure of nonsteroidal anti-inflammatory drugs to uncouple mitochondrial oxidative phosphorylation. *Biochem. Pharmacol.* **1999**, *58* (5), 861–5.
- (24) Mahmud, T.; Rafi, S. S.; Scott, D. L.; Wrigglesworth, J. M.; Bjarnason, I. Nonsteroidal anti-inflammatory drugs and uncoupling of mitochondrial oxidative phosphorylation. *Arthritis Rheum.* **1996**, *39* (12), 1998–2003.

(25) Tomoda, T.; Kurashige, T.; Hayashi, Y.; Enzan, H. Primary changes in liver damage by aspirin in rats. *Acta Paediatr. Jpn.* **1998**, *40* (6), 593–6.

(26) Somasundaram, S.; Rafi, S.; Hayllar, J.; Sigthorsson, G.; Jacob, M.; Price, A. B.; Macpherson, A.; Mahmood, T.; Scott, D.; Wrigglesworth, J. M.; Bjarnason, I. Mitochondrial damage: a possible mechanism of the "topical" phase of NSAID induced injury to the rat intestine. *Gut* **1997**, *41* (3), 344–53.

(27) Hasebe, T.; Harasawa, S.; Miwa, T.; Shibata, T.; Inayama, S. Collagen and collagenase in ulcer tissue-1. The healing process of acetic acid ulcers in rats. *Tokai J. Exp. Clin. Med.* **1987**, *12* (3), 147–58.

Pilot Study of Changes in Salivary Metabolic Profiles Induced by Template Therapy

SHOJI TANAKA¹, HITOSHI TAGA², KIYOSHI MAEHARA¹, AZUSA KANESHIMA^{1*},
MAMORU MACHINO¹, HIROMI ONUMA³, MIKU KANEKO³, HIROSHI SAKAGAMI¹,
MASAHIRO SUGIMOTO^{3,4}, TOMOYOSHI SOGA³ and MASARU TOMITA³

¹Meikai University School of Dentistry, Sakado, Japan;

²JR Tokyo General Hospital, Shibuya-ku, Tokyo, Japan;

³Institute for Advanced Biosciences, Keio University, Tsuruoka, Yamagata, Japan;

⁴Graduate School of Medicine and Faculty of Medicine, Kyoto University, Sakyo-ku, Kyoto, Japan

*Undergraduate student, Meikai University School of Dentistry

Abstract. *Background: Occlusal raising method (so-called 'Template therapy') has been reported to alleviate various diseases and symptoms, but the underlying mechanism is not clear. We searched the low-molecular weight metabolite(s) in the saliva, the concentration of which is significantly changed by the template therapy. Materials and Methods: One female patient with headache underwent the template therapy for 12 days, and her total saliva was subjected to non-targeted analysis using capillary electrophoresis time-of-flight mass spectrometry (CE-TOF-MS). Results: One hundred and thirteen substances were identified in the saliva. Glycine was the most abundant amino acid in the saliva, followed by alanine, serine and proline. After the start of the template therapy, her headache was alleviated, accompanied by a significant ($p=0.042$) increase of salivary concentration of glycine, as compared with total amino acids whereas that of other amino acids was not significantly changed. In the metabolomics profile, salivary concentration of large number of metabolites as compared with total metabolite concentration decreased, including N-acetylneuraminic acid ($p=0.025$) and p-hydroxyphenylacetate ($p=0.039$). Conclusion: This pilot study demonstrated, to our knowledge for the first time, that only glycine exhibited unique changes among total metabolites, suggesting its significant role in template therapy.*

There have been many clinical reports of various systemic symptoms such as headache, shoulder stiffness and mal-posture due to changes in the occlusal position (1-3). Several reports have attributed the artificial occlusal abnormalities to tooth extraction, bite raising and tooth grinding in experimental animals (4-9). These studies suggest that the trigeminal responses to occlusal changes induce various systemic symptoms by as yet -unidentified mechanisms. Out of these symptoms, the head drop and the drooping of the submandibular mental area to the ground were observed about one week after grinding the maxillary posterior teeth of guinea pigs to the cervical area. Abnormal waveforms including T-wave inversion were also observed on electrocardiogram (ECG) (9). We have recently reported that the decrease of the occlusal vertical dimension (OVD) in guinea pig models resulted in two-phase wave of heart rate fluctuations, with the first peak occurring 0-2 days after tooth grinding and the second peak starting from 4 days after teeth grinding until sudden death (usually 12th day), accompanied by the head drop, and that when the OVD was increased, such heart rate fluctuations disappeared (10). Although the occlusal raising method (the so-called 'Template therapy') has been reported to improve such systemic symptoms, the fundamental mechanism is not clear. In order to identify the biomarkers of compounds responsible for the efficacy of template therapy, we searched for low-molecular weight metabolites in the saliva, the concentration of which is significantly changed by template therapy, using capillary electrophoresis time-of-flight mass spectrometry (CE-TOF-MS).

Correspondence to: Shoji Tanaka, Division of Oral Diagnosis, Department of Diagnostic and Therapeutic Sciences, Meikai University School of Dentistry, 1-1 Keyakidai, Sakado, Saitama 350-0283, Japan. Tel: +81 492792758, Fax: +81 492855511, e-mail: stanaka@dent.meikai.ac.jp

Key Words: Template therapy, metabolite profiling, salivary glycine.

Materials and Methods

Sample collection. A female patient (30 years old) had headache or tension-type headache, low back pain and shoulder stiffness, and had a medical examination in Maehara Dental Clinic, Shinjuku-